

Multi-criticality and related bifurcation in accretion discs around non-rotating black holes – an analytical study

Arpan Krishna Mitra^{1*}, Aishee Chakraborty^{1†}, Pratik Tarafdar^{2‡},
Tapas Kumar Das^{1,3§}

¹Harish Chandra Research Institute, Chhatnag Rd, Jhansi
Prayagraj 211019, Uttar Pradesh, India.

²The Institute of Mathematical Sciences, IV Cross Road, CIT Campus,
Taramani, Chennai 600113, Tamil Nadu, India.

³Homi Bhabha National Institute, Training School Complex,
Anushakti Nagar, Mumbai 400094, Maharashtra, India.

Abstract

Low angular momentum, general relativistic, axially symmetric accretion of hydrodynamic fluid onto Schwarzschild black holes may undergo more than one critical transition. To obtain the stationary integral solutions corresponding to such multi-critical accretion flow, one needs to employ numerical solutions of the corresponding fluid dynamics equations. In the present work, we develop a completely analytical solution scheme which may be used to find several trans-critical flow behaviours of aforementioned accretion, without explicitly solving the flow equations numerically. We study all possible geometric configurations of the flow profile, governed by all possible thermodynamic equations of state. We use Sturm's chain algorithm to find out

*E-mail: arpankrishnamitra@hri.res.in

†E-mail: aisheechakraborty@hri.res.in

‡E-mail: pratikt@imsc.com

§E-mail: tapas@hri.res.in

how many physically acceptable critical points the accretion flow can have, and discuss the transition from the mono to the multi-critical flow profile, and related bifurcation phenomena. We thus illustrate, completely analytically, the application of certain aspects of the dynamical systems theory in the field of large scale astrophysical flow under the influence of strong gravity. Our work may possibly be generalized to calculate the maximal number of equilibrium points certain autonomous dynamical systems can have in general.

1 Introduction

The accretion process towards astrophysical black holes almost always exhibit transonicity¹ in order to satisfy the inner boundary conditions imposed by the event horizon. Recent studies have concluded that, low angular momentum axially symmetric sub-Keplerian accretion flow shows multi-transonicity as well [1]. Apart from this multi-transonic behaviour, we can demonstrate this whole accretion as a dynamical system and can draw a phase portrait where the transonic points are realized mathematically as the critical points of phase flow [2, 3, 4, 5, 6, 7, 8, 9, 10, 11, 12, 13]. For certain astrophysically relevant boundary conditions, the flow can have a maximum of three critical points, of which two are saddle-type critical points and the third one is a centre-type critical point, which is attenuated between the previous two. So, a complete study of low angular momentum axially symmetric sub-Keplerian accretion onto astrophysical black holes, necessitates an exact solution of the two fundamental fluid dynamic equations (Euler and continuity equation). But the equations are not exactly solvable analytically due to their inherent nonlinear nature. In order to get around this difficulty, we need to resort to alternative numerical methods [18, 20, 22, 23, 24, 25, 26, 27, 28, 31, 32, 33]. Aforementioned papers have already solved them numerically and described the whole process from a semi-analytical approach. Very recently, a technique is developed [14] using Sturm analysis which gives us exact number of physically acceptable solutions (for which the critical points form outside the horizon) of a n -th order algebraic polynomial(of critical points) for a set of initial conditions. So, this method will help us to investigate the multi-transonicity of a general relativistic flow onto a Schwarzschild black hole completely analytically, and to get a real flavour of multi-transonic

¹except when the accreting matter starts supersonically from a reasonably large distance.

accretion flow features without numerical computations. In this paper, we will focus on providing an entirely analytical qualitative visualization for a generalised flow structure, using Sturm method. Here, we first have to construct an equation involving the spatial gradient of the advective velocity of accreting matter. Afterwards, by equating the expression for spatial gradient of the same, we obtain an algebraic polynomial equation for the critical spatial variable(r_c) upon which Sturm analysis will be applied later to get the exact number of solutions in the astrophysically relevant region outside the event horizon. We will further demonstrate through bifurcation diagrams, the transition from mono to multitransonicity upon variation of system parameters.

We have organized our paper as follows, after a brief introductory section we will discuss about the background spacetime structure over which the accretion occurs, and about the quantities which remains conserved during the flow. In the third section we will present a brief description of existing models of accretion discs. In subsequent two chapters we will focus on the properties of accretion on these models where the flow is polytropic and isothermal in nature respectively and will discuss about the multi-criticality of the flows and related bifurcation phenomena. We will add some concluding remarks regarding the novelty and the scope of this venture.

2 Background space-time geometry and the first integrals of motion

We consider the disc accretion to occur in a (3+1) stationary axially symmetric space-time having two killing vectors commuting with each other. The local time-like killing vector $\xi^\mu \equiv (\frac{\partial}{\partial t})^\mu$ plays the role of generator of the stationary behaviour while $\phi^\mu \equiv (\frac{\partial}{\partial \phi})^\mu$ generates the axial symmetry. We have done all the measurements in natural units($G=c=1$). M_{bh} , the black hole mass, is scaled to 1. We consider the energy momentum tensor of an ideal fluid

$$T^{\mu\nu} = (\epsilon + p)u^\mu u^\nu + pg^{\mu\nu}$$

defined in a space time. Such a space time is described by cylindrical Boyer-Lindquist coordinate in equatorial plane ($z = 0$) as defined below:

$$ds^2 = g_{\mu\nu}dx^\mu dx^\nu = -\frac{r^2\Delta}{A}dt^2 + \frac{A}{r^2}(d\phi - \omega dt)^2 + \frac{r^2}{\Delta}dr^2 + dz^2 \quad (1)$$

where

$$\Delta = r^2 - 2r + a^2, \quad A = r^4 + r^2 a^2 + 2ra^2, \quad \omega = \frac{2ra}{A}$$

When we consider accretion on Schwarzschild BH (non-rotating), we set the Kerr parameter $a = 0$. With this condition, we have,

$$\Delta = r(r - 2), \quad A = r^4, \quad \text{and} \quad \omega = 0.$$

The metric components are then given as,

$$g_{rr} = \frac{r}{(r - 2)}, \quad g_{tt} = -\frac{(r - 2)}{r}, \quad g_{\phi\phi} = r^2, \quad g_{t\phi} = g_{\phi t} = 0. \quad (2)$$

2.1 First integrals of motion

We have two types of accretion flow governed by two different thermodynamic equations of state, namely, the polytropic, in which the energy conservation holds and the isothermal, i.e. a constant temperature flow. The relativistic Euler equation for polytropic accretion is found from the conservation equation of the EM tensor,

$$T^{\mu\nu}_{;\nu} = 0. \quad (3)$$

On top of that we have another conservation equation, namely the continuity equation

$$(\rho u^\mu)_{;\mu} = 0 \quad (4)$$

in fluid context.

2.1.1 Integral solution of the linear momentum conservation equation

Contraction of the equation (3) with the specified Killing vectors ϕ^μ and ξ^μ produces angular momentum per baryon hu_ϕ and relativistic Bernoulli's constant hu_t (h is the specific enthalpy of the system) respectively, which can be shown to be conserved. It can be identified with \mathcal{E} the total specific energy of the ideal GR fluid scaled in units of the rest-mass energy.

We define the specific angular momentum (λ) and the angular velocity (Ω) as,

$$\lambda = -\frac{u_\phi}{u_t} \quad (5)$$

$$\Omega = \frac{u^\phi}{u^t} = -\frac{g_{t\phi} + \lambda g_{tt}}{g_{\phi\phi} + \lambda g_{t\phi}} \quad (6)$$

Using the normalization condition $u^\mu u_\mu = -1$ we obtain,

$$u_t = \sqrt{\frac{g_{t\phi}^2 - g_{tt}g_{\phi\phi}}{(1 - \lambda\Omega)(1 - u^2)(g_{\phi\phi} + \lambda g_{t\phi})}} \quad (7)$$

The corresponding expression for conserved energy \mathcal{E} is therefore given by,

$$\mathcal{E} = \frac{\gamma - 1}{\gamma - (1 + c_s^2)} \sqrt{\frac{g_{t\phi}^2 - g_{tt}g_{\phi\phi}}{(1 - \lambda\Omega)(1 - u^2)(g_{\phi\phi} + \lambda g_{t\phi})}} \quad (8)$$

It is evident that the specific energy is independent of the matter(disc) geometry but depends on the space time geometry.

In case of isothermal accretion, energy dissipation occurs to maintain a constant temperature. Hence, the total energy cannot be conserved. However we may derive a conserved quantity upon integration of the relativistic Euler equation, which is different from the total energy of the system.

The isotropic pressure is directly proportional to the specific energy of the fluid

$$p = c_s^2 \epsilon \quad (9)$$

The energy-momentum conservation equation we obtain by setting the 4-divergence (covariant derivative w.r.t. ν) of (3) to be zero is,

$$p_{,\nu}(g^{\mu\nu} + u^\mu u^\nu) + u^\nu u^\mu_{;\nu} = 0 \quad (10)$$

Using (9) we get the general relativistic Euler equation for isothermal accretion.

$$\frac{c_s^2}{\rho} \rho_{,\nu}(g^{\mu\nu} + u^\mu u^\nu) + u^\nu u^\mu_{;\nu} = 0 \quad (11)$$

We introduce the irrotationality condition here, $\omega_{\mu\nu} = 0$ with, $\omega_{\mu\nu} = l_\mu^\alpha l_\nu^\beta v_{[\alpha;\beta]}$. Here, $l_\mu^\alpha = \delta_\mu^\alpha + u^\alpha u_\mu$ is the projection operator acting in the normal direction of u^μ , and $u_{[\alpha;\beta]} = \frac{1}{2}(u_{\beta;\alpha} - u_{\alpha;\beta})$. With this condition fed into (11) we have

$$\partial_\nu(u_\mu \rho c_s^2) - \partial_\mu(u_\nu \rho c_s^2) = 0 \quad (12)$$

The time component of (12) shows, for isothermal irrotational flow, $(u_t \rho c_s^2) = C_{iso}$ is found to be a conserved quantity. Hence, C_{iso} is the first integral in isothermal accretion, which should not be identified with the specific energy of the system.

2.1.2 Integral solution of the mass conservation equation

The continuity equation (4) gives us,

$$\frac{1}{\sqrt{-g}}(\sqrt{-g}\rho u^\mu)_{,\mu} = 0, \quad (13)$$

where $g \equiv \det(g_{\mu\nu})$. We now have,

$$d^4x(\sqrt{-g}\rho u^\mu)_{,\mu} = 0 \quad (14)$$

with $\sqrt{-g}d^4x$ be the covariant volume element. The z component of the velocity u^z (in cylindrical coordinates) or the polar component u^θ (in spherical polar coordinates) are assumed to be negligible w.r.t the transformed radial component u^r . With this assumption we have,

$$\partial_r(\sqrt{-g}\rho u^r)drd\theta d\phi = 0; \quad \partial_r(\sqrt{-g}\rho u^r)drdzd\phi = 0 \quad (15)$$

for stationary flow in spherical and cylindrical polar coordinates respectively. The equation for spherical polar coordinates is integrated for ϕ from 0 to 2π and θ from $-H_\theta$ to H_θ , $\pm H_\theta$ being the corresponding values of the coordinates above and below the equatorial plane respectively, for local half thickness H , to obtain the conserved quantity \dot{M} , the mass accretion rate when $\theta = \frac{\pi}{2}$ (i.e. on the equatorial plane). The mass accretion rate \dot{M} depends on the matter geometry configurations. We here present a general expression for it.

$$\dot{M} = \rho u^r \mathcal{A}(r) \quad (16)$$

where $\mathcal{A}(r)$ stands for the $2D$ surface area through which the steady state inbound mass flux is calculated.

3 Disc geometries

We here follow the footsteps of the existing literature to assume that the axially symmetric accretion flow has a radius dependent local thickness $H(r)$, and the central plane of the flow coincides with the equatorial plane of the black hole.

3.1 Flow with a Constant Height:

For constant height (CH hereafter) flows, height or half-thickness (H) of accretion disc is constant throughout. H doesn't depend on the radial distance.

$$H(r) = \text{constant} \quad (17)$$

3.2 Quasi-spherical Flow:

In case of quasi-spherical (qu hereafter) flows the flow geometry obeys the conical structure resembling a sphere with cones scooped out from opposite poles. The height(H) of the disc varies linearly with radial distance(r).

$$H = r\Lambda_a \quad (18)$$

Λ_a is the angle subtended by the conical flow at the event horizon which is approximately constant throughout the flow.

3.3 Flow with Hydrostatic Equilibrium in Vertical Direction:

In this model, it is customary to average out physical variables associated with flow (such as pressure(P), density(ρ) etc.) [24, 34, 51, 52, 53, 54, 55, 56, 57, 58, 59, 62] to an approximately constant value for a definite disc height H at a definite radial distance from the event horizon. This model can be classified into three subdivisions:

3.3.1 Novikov-Thorne Model:

The structure of disc height or half-thickness $H(r)$ for this Novikov-Thorne model [15] (NT hereafter) is given by,

$$H(r) = \left(\frac{P}{\rho}\right)^{\frac{1}{2}} r^{\frac{3}{2}} \left(1 - \frac{3}{r}\right) \left(1 - \frac{2}{r}\right)^{-\frac{1}{2}} \quad (19)$$

3.3.2 Riffert-Herold Model:

For this Riffert-Herold model[16] (RH hereafter) the half thickness or height of the disc H is given by,

$$H(r) = 2 \left(\frac{P}{\rho}\right)^{\frac{1}{2}} r^{\frac{3}{2}} \sqrt{1 - \frac{3}{r}} \quad (20)$$

3.3.3 Abramowicz-Lanza-Percival Model:

The height or half-thickness of the disc, H for this Abramowicz-Lanza-Percival Model [17] (ALP hereafter) is given by:

$$H(r) = \frac{r^2 c_s}{\lambda} \sqrt{\frac{2(1-u^2)(1 - \frac{\lambda^2}{r^2}(1 - \frac{2}{r}))(\gamma - 1)}{\gamma(1 - \frac{2}{r})(\gamma - (1 + c_s^2))}} \quad (21)$$

In general, low angular momentum accretion flow don't predict thin disc structure of flow and from that perspective, conical flow structure is approximately more convenient over the flow model in hydrostatic equilibrium in vertical direction. Although, we will present here a detailed description qualitatively for the all five flow geometries to generalise the sturm analysis.

4 Polytropic accretion

The equation of state governing a polytropic fluid is given by,

$$p = K \rho^\gamma, \quad (22)$$

where p is the pressure of the accreting fluid, γ is the polytropic index which is assumed to be constant throughout the accretion process² and K gives us the measure of specific entropy, provided, no additional generation of entropy occurs in the process. Specific enthalpy can be formulated as,

$$h = \frac{\epsilon + p}{\rho} \quad (23)$$

with, ϵ being the internal energy density of the system measured by the relation

$$\epsilon = \rho + \frac{p}{\gamma - 1} \quad (24)$$

The speed of sonic propagation in an adiabatic process is obtained as,

$$c_s^2 = \left(\frac{\partial p}{\partial \epsilon} \right) \Big|_h \quad (25)$$

²it is the ratio of the specific heats $\frac{C_p}{C_v}$

Simple manipulation of (24) and (25) gives,

$$\rho = \left(\frac{c_s^2(\gamma - 1)}{\gamma K(\gamma - 1 - c_s^2)} \right)^{\frac{1}{\gamma-1}} \quad (26)$$

In polytropic accretion process we have two first integrals of motion, firstly, the conserved specific energy \mathcal{E} , and the mass accretion rate \dot{M} . Which are given by,

$$\mathcal{E} = \frac{(\gamma - 1)r}{\gamma - 1 - c_s^2} \sqrt{\frac{(r - 2)}{(1 - u^2)(r^3 - \lambda^2(r - 2))}} \quad (27)$$

$$\dot{M} = \rho v^r A(r) \quad (28)$$

This energy expression we obtain by integrating the stationary part of the Euler equation holds good for all the accretion disc geometries. On the other hand, the mass accretion rate obtained by integrating the stationary part of the continuity equation is explicitly dependent on the specific disc geometry.

We are going to calculate the radial derivative of the dynamical velocity u for different disc geometries, and will be representing them in \mathcal{N}/\mathcal{D} form. For a physically realisable transonic flow, $\frac{du}{dr}$ has to be smooth at every point inside the astrophysical domain. Now, at the critical points, $\frac{du}{dr}$ can assume multiple values depending on the specific set of system parameters. In other words, the spatial derivative of dynamical velocity becomes undefined, i.e. $\mathcal{D} = 0$. However, using the aforesaid logic for smooth flows, \mathcal{N} should also be zero at critical points. Hence the condition $\mathcal{N} = \mathcal{D} = 0$ leads us to the criticality conditions. This condition when fed into (27) gives us the required polynomial equation whose solutions represent the critical points (r_c).

Now, these polynomials as will be shown in the subsequent sections are usually (except in a few special cases) of order $n > 4$ and hence, not analytically solvable. So, in order to obtain the number of real roots of the polynomial equations for a specified range of parameters within relevant astrophysical domain³, we need to use the Sturm method that we discussed earlier ([14]).

4.1 Constant Height Model

The mass accretion rate for this specific disc geometry (using (28)) is given by

³[1 $\lesssim \mathcal{E} \lesssim 2, 0 \leq \lambda \leq 2, 4/3 \leq \gamma \leq 5/3$][26]

$$\dot{M} = 2\pi\rho \frac{u\sqrt{1-\frac{2}{r}}}{\sqrt{1-u^2}} rH \quad (29)$$

which is assumed to be constant throughout the flow.

These two equations (27) and (29) contain three unknown quantities ρ , u , and c_s , which are functions of r . Hence, one needs to eliminate one of the three by expressing it in terms of the other two. We here, would like to express ρ in terms of u and c_s , as we are interested in studying the profile for the radial Mach number $M_c = \frac{u}{c_s}$ to get the location of the acoustic horizons (i.e. the radial positions where M_c is unity). For this purpose, we make use the transformation-

$$\dot{\mathcal{M}} = \dot{M}(K\gamma)^{\frac{1}{\gamma-1}} \quad (30)$$

$\dot{\mathcal{M}}$ may be interpreted as a measure of the net inbound entropy flux of the fluid and hence, can be defined as the stationary entropy accretion rate. This entropy accretion rate was proposed for the first time in [18, 19].

Using (30), (29) and (27) following the aforementioned pathway we derive an expression of $\frac{du}{dr}$ which looks like,

$$\frac{du}{dr} = \frac{c_s^2(\frac{r-1}{r(r-2)}) - f(r, \lambda)}{\frac{u^2 - c_s^2}{u(1-u^2)}} = \frac{\mathcal{N}}{\mathcal{D}} \quad (31)$$

where,

$$f(r, \lambda) = \frac{r^3 - \lambda^2(r-2)^2}{r(r-2)(r^3 - \lambda^2(r-2))} \quad (32)$$

Inspecting the denominator \mathcal{D} we can readily conclude that the critical point coincides with the sonic point here, as,

$$\mathcal{D} = 0 \implies u|_{r_c} = c_s \quad (33)$$

and, dictated by the argument that u has to be a smooth function of the radial distance, we have $\mathcal{N} = 0$ at the critical point. The advective velocity and/or the local sound speed at the critical point can be calculated from this condition.

$$u_c = c_{s|c} = \sqrt{\frac{f(r, \lambda)}{\frac{r-1}{r(r-2)}}}|_{r_c} \quad (34)$$

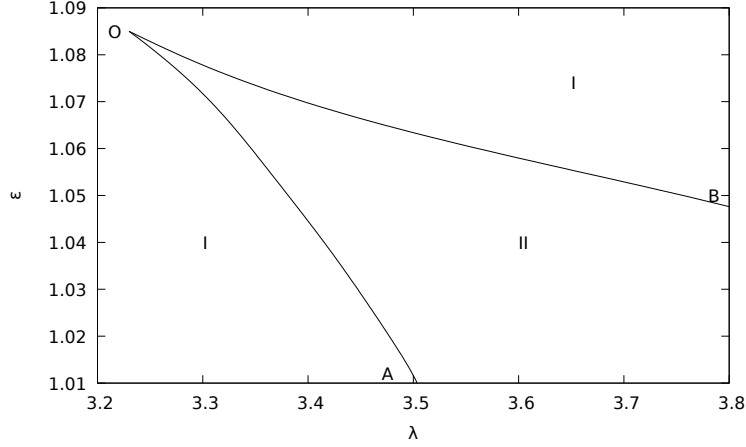


Figure 1: Polytropic accretion in constant height discs and related bifurcation phenomena

When (34) is fed in (27) it produces a $\mathcal{O}(\sim 11)$ polynomial equation in r_c ⁴.

$$\sum_{i=0}^{11} a_{chi} r_c^i = 0 \quad (35)$$

Here, the number of critical points is equal to the number of real roots of the above polynomial equation. Now, applying Sturm analysis on the above polynomial equation, for the region $r=3.1r_s$ to $10,000r_s$ (where r_s denotes the Schwarzschild radius), we obtain the number of real roots in a certain range of λ and \mathcal{E} . The corresponding bifurcation diagram to describe the flow qualitatively in λ – \mathcal{E} space has been shown in 1.

In 1, region I denotes the mono-critical region where only one critical point exists and region II denotes the multi-critical region where three critical points exist. Here, OA and OB curves separate these two regions from one another. The interior of the region OAB (bounded by OA and OB curves) specifies the multi-critical region II. For example, at $\mathcal{E} = 1.06$, in the range of $\lambda \leq 3.33$ (region I) there is a mono-critical solution of $f(r_c)$ and in the range $3.33 \leq \lambda \leq 3.55$ there is a multi-critical solution of $f(r_c)$ (region II) and in the range $\lambda \geq 3.55$ there again exist mono-critical solutions of $f(r_c)$ (region I). Basically at first, in region I (upto $\lambda = 3.51$), there exists only one real root, which means there is a saddle point through which the physical flow occurs. At $\lambda = 3.33$, that saddle point splits into two different saddle points and in between these two, a center type critical point is created. As a result, we get the number of real roots as 3. This continues up to $\lambda = 3.55$ (region II). After λ attains a value

⁴for the coefficients of the polynomial see **Appendix 2**

3.55, the inner saddle point and center type critical point goes beyond our inner limit of radial distance r and only one critical point (outer saddle point) is left. So, we get back a mono-critical region (region I). This saddle-node bifurcation occurs for each and every value of \mathcal{E} in the given range of \mathcal{E} in a similar manner. Thus accretion flow continues from a distant region to close proximity of the event horizon and then finally falls onto the black hole.

4.2 Quasi-spherical Flow

For mass accretion rate in a quasi spherical flow we use (28) and (18) to obtain,

$$\dot{M} = \Lambda_{iso} \rho \frac{u \sqrt{1 - \frac{2}{r}}}{\sqrt{1 - u^2}} r^2 \quad (36)$$

From (30), (36) and (27), and finally using (32) we arrive at the following expression,

$$\frac{du}{dr} = \frac{c_s^2 \left(\frac{2r-3}{r(r-2)} \right) - f(r, \lambda)}{\frac{u^2 - c_s^2}{u(1-u^2)}} = \frac{\mathcal{N}}{\mathcal{D}} \quad (37)$$

Now as u is a smooth function of r , null value of the denominator at some point in the range implies that the numerator has to be zero simultaneously, which in turn gives us the mathematical condition for critical points.

Inspecting the denominator \mathcal{D} we can readily conclude that the critical point coincides with the sonic point in this case as well,

$$\mathcal{D} = 0 \implies u|_{r_c} = c_s \quad (38)$$

Again following the same argument as in the previous case, we have $N = 0$ at the critical point. Hence, the advective velocity and/or the local sound speed at the critical point can be calculated from this condition.

$$u_c = c_{s|c} = c_s = \sqrt{\frac{f(r, \lambda)}{\frac{2r-3}{r(r-2)}}}|_{r_c} \quad (39)$$

When (34) is fed into (27) it produces a $\mathcal{O}(\sim 11)$ polynomial equation in r_c .⁵

$$\sum_{i=0}^{11} a_{qi} r_c^i = 0 \quad (40)$$

⁵for the coefficients of the polynomial see **Appendix 3**

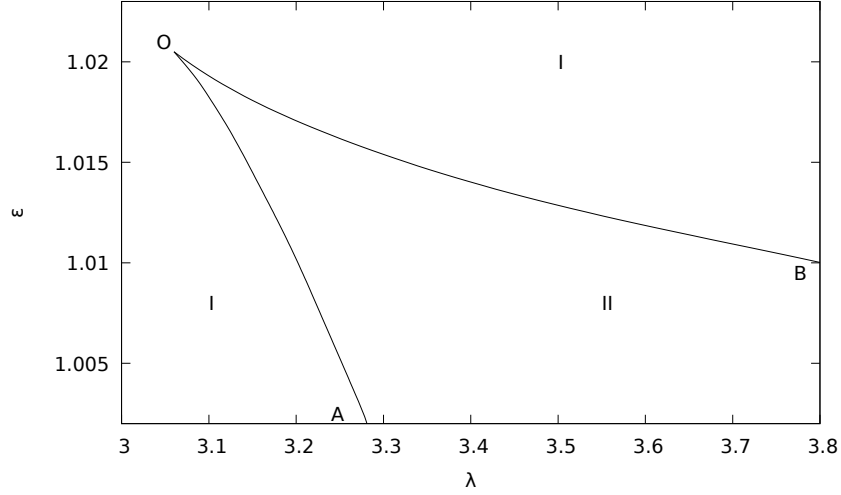


Figure 2: Polytropic accretion in conical discs and related bifurcation phenomena

Here, the number of critical points is equal to the number of real roots of the above polynomial equation. Now applying Sturm analysis on the above polynomial, for the region $r=3.1r_s$ to $10,000r_s$ (where r_s denotes the Schwarzschild radius), we obtain the number of real roots in a certain range of λ and \mathcal{E} . The bifurcation diagram to describe the flow qualitatively in λ - \mathcal{E} space is shown in 2.

In 2, the region I denotes the mono-critical region and region II denotes the multi-critical region. Curve OA and OB represents the left and right boundary (between region I to II). The interior of the wedge shaped region OAB specifies the multi-critical region II. For example, at $\mathcal{E} = 1.014$, in the range of $\lambda \leq 3.16$ (region I) there exists only one physically acceptable solution $f(r_c)$ and in the range $3.16 \leq \lambda \leq 3.58$ there are three such solutions of $f(r_c)$ (region II) and in the range $\lambda \geq 3.58$ there again exists one physical solution of $f(r_c)$ (region I).

4.3 Flow in vertical hydrostatic equilibrium

4.3.1 Novikov-Thorne Accretion Flow Model

Here the mass accretion rate is given by,

$$\dot{M} = 4\pi\rho r \frac{u\sqrt{1-\frac{2}{r}}}{\sqrt{1-u^2}} H_{NT}(r). \quad (41)$$

Using the expression of height of accreting disc $H_{NT}(r)$, given in (19)

$$\dot{M} = 4\pi\rho c_s r^{\frac{5}{2}} \frac{u\sqrt{1-\frac{3}{r}}}{\sqrt{1-u^2}} \quad (42)$$

From (30), (42), (8) and (32) we get the following expression for $\frac{du}{dr}$:

$$\frac{du}{dr} = \frac{c_s^2 \left(\frac{5r-12}{r(r-3)(\gamma+1)} \right) - f(r, \lambda)}{\frac{u^2(\gamma+1)-2c_s^2}{u(1-u^2)(\gamma+1)}} = \frac{\mathcal{N}}{\mathcal{D}} \quad (43)$$

We use the same argument of $u(r)$ being a smooth function of r to obtain the critical point conditions,

$$u|_{r_c} = \sqrt{\frac{2}{\gamma+1} c_s}|_{r_c}, \quad (44)$$

$$c_s = \sqrt{\frac{f(r, \lambda)}{\frac{5r-12}{r(r-3)(\gamma+1)}}}|_{r_c}. \quad (45)$$

When (45) is fed into (27) it produces a $\mathcal{O}(\sim 15)$ polynomial equation in r_c ⁶.

$$\sum_{i=0}^{15} a_{NT,i} x^i = 0 \quad (46)$$

Here we know that, the number of critical points equals to the number of real roots of the polynomial. Now applying Sturm analysis on the derived polynomial equation for the region $r=3.1r_s$ to $10,000r_s$, we compute the bifurcation diagram in λ - \mathcal{E} space to describe the accretion flow qualitatively. The respective diagram is shown in the 3.

In 3, the region I denotes the mono-critical region where only one critical point exists and region II denotes the multi-critical region where three critical points exist. Here, OA and OB curves represent the left boundary the right boundary(between region II to I). The bounded area OAB presents the multi-critical region II. As an example, we consider a particular value of specific energy $\mathcal{E} = 1.012$, in the range of $\lambda \leq 3.02$ (region I) there is a mono-critical solution of $f(r_c)$ and in the range $3.02 \leq \lambda \leq 3.19$ there is a multi-critical solution

⁶for the coefficients of the polynomial see **Appendix 4**

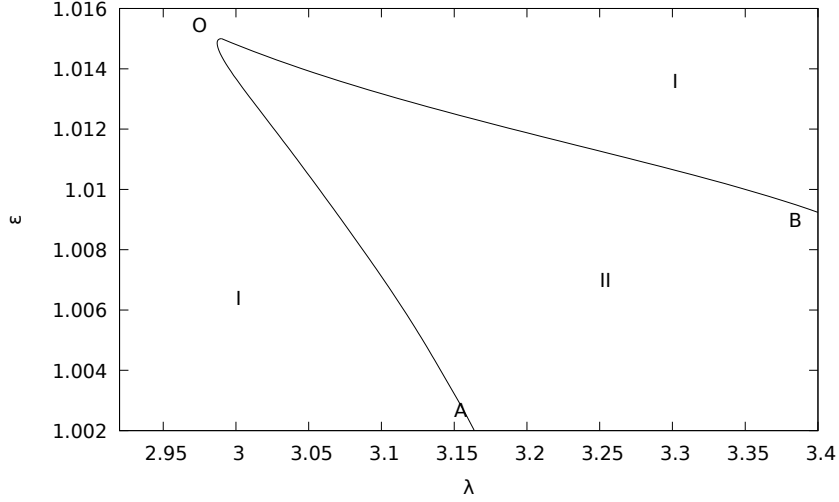


Figure 3: Polytropic accretion in NT flow model and related bifurcation phenomena

of $f(r_c)$ (region II) and in the range $\lambda \geq 3.19$ there again exists a mono-critical solution of $f(r_c)$ (region I).

4.3.2 Riffert-Herold Accretion Flow Model

Here, mass accretion rate is given by,

$$\dot{M} = 4\pi\rho r \frac{u\sqrt{1-\frac{2}{r}}}{\sqrt{1-u^2}} H(r) \quad (47)$$

Now, substituting the expression of $H(r)$ from (20) into (47), we obtain the final expression of mass accretion rate:

$$\dot{M} = 8\pi\rho c_s r^{\frac{5}{2}} \frac{u\sqrt{(1-\frac{2}{r})(1-\frac{3}{r})}}{\sqrt{1-u^2}} \quad (48)$$

(which remains approximately constant throughout the flow).

From (30), (48), (27) and (32) we obtain the expression for $\frac{du}{dr}$ as,

$$\frac{du}{dr} = \frac{c_s^2(\frac{5r^2-20r+18}{r(r-2)(r-3)(\gamma+1)}) - f(r, \lambda)}{\frac{u^2(\gamma+1)-2c_s^2}{u(1-u^2)(\gamma+1)}} = \frac{\mathcal{N}}{\mathcal{D}} \quad (49)$$

In the equation(27), equating $\mathcal{D} = 0$, we obtain the equation connecting the local advective velocity with the local sonic speed at the critical radius r_c .

$$u|_{r_c} = \sqrt{\frac{2}{\gamma+1}} c_s|_{r_c} \quad (50)$$

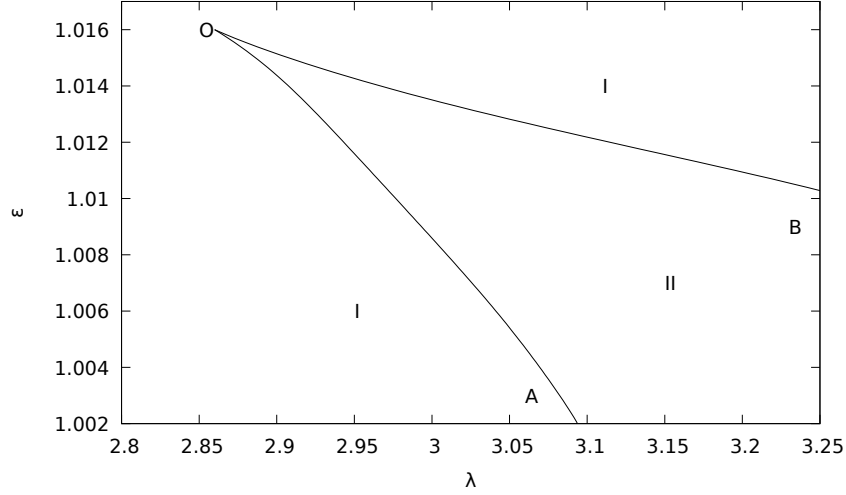


Figure 4: Polytropic accretion in RH flow model and related bifurcation phenomena

and the other critical point condition $\mathcal{N} = 0$, gives us,

$$c_s = \sqrt{\frac{f(r, \lambda)}{\frac{5r^2 - 20r + 18}{r(r-2)(r-3)(\gamma+1)}}} \quad (51)$$

This result in (27) generates a polynomial equation $O(\sim 14)$ in critical radius.

$$\sum_{i=0}^{14} a_{RH_i} x^i = 0 \quad (52)$$

We know that, the number of critical points is equal to the number of real roots of the above polynomial equation. Now applying Sturm analysis on the derived polynomial for the region $r=3.1r_s$ to $10,000r_s$, we obtain a bifurcation diagram in λ - \mathcal{E} space to describe the accretion flow qualitatively. The respective diagram is shown in the 4.

In 4, the region I denotes the mono-critical region where only one critical point exists and region II denotes the multi-critical region where three critical points exist. Here, OA curve represents the left boundary and curve OB represents the right boundary (between region I to II). Interior of the OAB region(bounded by OA and OB) depicts the multi-critical region II. Now, for example, at $\mathcal{E} = 1.012$, in the range of $0 \leq \lambda \leq 2.93$ (region I) there is a mono-critical solution of $f(r_c)$ and in the range $2.93 \leq \lambda \leq 3.11$ there is a multi-critical solution of $f(r_c)$ (region II) and in the range $3.79 \leq \lambda \leq 4.0$ there again exists a mono-critical solution of $f(r_c)$ (region I).

Table 1: Bifurcation region for polytropic accretion

Disc geometry	λ	\mathcal{E}	γ
CH	3.50-3.80	1.01 – 1.085	$\frac{5}{3}$
Quasi-spherical	3.28-3.80	1.00 – 1.021	$\frac{5}{3}$
NT	3.16-3.40	1.002 – 1.016	$\frac{5}{3}$
RH	3.09 - 3.25	1.002 – 1.018	$\frac{5}{3}$

5 Isothermal Accretion Flow

Here we are going to discuss multicritical accretion which may contain more than one critical points throughout the flow. We know that in isothermal flow, temperature T remains constant. Hence, the specific energy can no longer be a conserved quantity due to continuous energy exchange with surroundings. In this case, the conserved quantities are specific angular momentum (λ) and another quantity (ξ), namely quasi-specific energy, which may be derived from integration of the stationary part of the relativistic Euler's equation. The expression for this ξ is given by,

$$\xi = \frac{r^2(r-2)}{(r^3 - \lambda^2(r-2))(1-u^2)} \rho^{2c_s^2} \quad (53)$$

Here, ρ is the density of the accreting fluid; \mathbf{r} is the radial distance of accreting material from the event horizon ; \mathbf{u} is the advective velocity which has to be a smooth function of the radial distance in order to get a physically relevant accretion flow and c_s^2 is the local sound speed. Here, in isothermal accretion, the equation of state for the accreting fluid is:

$$P = \frac{\kappa_B}{\mu m_H} \rho T \quad (54)$$

with m_H representing the mass of proton and μ , the mean molecular mass of the ionised hydrogen.

We know for the isothermal case, $\frac{P}{\rho} = c_s^2$. So,

$$c_s^2 = \frac{\kappa_B}{\mu m_H} T \quad (55)$$

5.1 Flow with Constant Height H

The mass accretion rate for this constant height geometry is:

$$\dot{M} = 2\pi\rho \frac{u\sqrt{1-\frac{2}{r}}}{\sqrt{1-u^2}} rH \quad (56)$$

which remains constant throughout the flow as per our assumptions. From (53) and (56), using the previously elaborated methodology, we arrive at the following expression for $\frac{du}{dr}$,

$$\frac{du}{dr} = \frac{u(u^2-1)[2r^3-2\lambda^2(r-2)^2+c_s^2(2r^3-2\lambda^2r+4\lambda^2)(1-r)]}{r(2-r)(u^2-c_s^2)(2\lambda^2r-4\lambda^2-2r^3)} = \frac{\mathcal{N}}{\mathcal{D}} \quad (57)$$

As u is a continuous function of r , if the value of denominator \mathcal{D} be zero at some radial distance within the range of physical interest, then at those point, numerator \mathcal{N} has to be zero, which actually gives us the required critical condition. Here, null value of denominator \mathcal{D} tells us that, for this CH model critical point coincides with sonic point:

$$u|_{r_c} = c_s \quad (58)$$

Now at sonic point, numerator \mathcal{N} has to be zero and so the value of advective velocity at critical point is given by,

$$u_c = c_s|_{r_c} = \sqrt{\frac{2\lambda^2(r-2)^2-2r^3}{(2r^3-2\lambda^2r+4\lambda^2)(1-r)}} \quad (59)$$

Simplifying the above expression (59) we get a polynomial equation in r_c of order 4 as:

$$f(r_c) = 2c_s^2r_c^4 - 2(1+c_s^2)r_c^3 - 2\lambda^2(c_s^2-1)r_c^2 + 2\lambda^2(3c_s^2-4)r_c - 4\lambda^2(c_s^2-2) \quad (60)$$

Now the number of critical points is equal to the number of real roots of the above polynomial (60). Applying Sturm analysis on the above polynomial, for the region $r=3.1r_s$ to $10,000r_s$ (where r_s denotes the Schwarzschild radius), we have got the number of real roots in a certain range of λ and T and drawn a bifurcation diagram in λ - T space to describe the flow qualitatively. The respective diagram is shown in the 5.

In 5, the region I denotes the mono-critical region where only one critical point exists and region II denotes the multi-critical region where three critical points exist. Here, OA line represents the left boundary (from region I to II) and OB line represents the right boundary (from region II to I). OAB region (bounded by OA and OB lines) specifies the multi-critical region

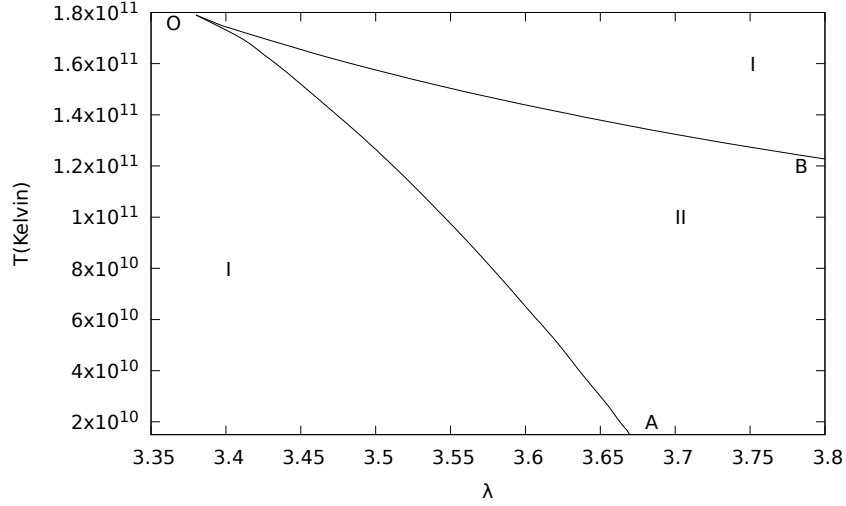


Figure 5: Isothermal accretion in constant height discs and related bifurcation phenomena

II. Now, for example, at $T = 1.2 \times 10^{11}$, in the range of $0 \leq \lambda \leq 3.51$ (region I) there is a mono-critical solution of $f(r_c)$ and in the range $3.51 \leq \lambda \leq 3.84$ there is a multi-critical solution of $f(r_c)$ (region II) and in the range $3.84 \leq \lambda \leq 4.0$ there again exists a mono-critical solution of $f(r_c)$ (region I). Here basically at first in region I (upto $\lambda = 3.51$), there exists only one real root which means, there is a saddle point through which accretion flow occurs. At $\lambda = 3.51$, that saddle point breaks into two different saddle points and in between these two, another critical point is created. As a result, we get the number of real roots 3. This continues upto $\lambda = 3.84$ (region II). After λ attains a value 3.84, one of those two saddle points and another critical point goes beyond our taken range of radial distance r and only one critical point (saddle node) is left. So, again we get a mono-critical region (region I). This saddle node bifurcation occurs for each and every value of T in the given range of T in a similar manner. Thus accretion flow continues from a distant region to very close to the event horizon and then finally falls on the black hole.

5.2 Quasi-Spherical Flow

The mass accretion rate of this accretion flow geometry is given by,

$$\dot{M} = \Lambda_{iso} \rho \frac{u \sqrt{1 - \frac{2}{r}}}{\sqrt{1 - u^2}} r^2 \quad (61)$$

(Λ_{iso} is a geometrical solid angle factor for this flow) which is assumed to be constant throughout the flow.

From the expression of (53) and (61), by similar procedure as previous, we get an expression of $\frac{du}{dr}$ as:

$$\frac{du}{dr} = \frac{u(u^2 - 1)[2r^3 - 2\lambda^2(r - 2)^2 + c_s^2(2r^3 - 2\lambda^2r + 4\lambda^2)(3 - 2r)]}{r(2 - r)(u^2 - c_s^2)(2\lambda^2r - 4\lambda^2 - 2r^3)} = \frac{\mathcal{N}}{\mathcal{D}} \quad (62)$$

Here, we will use the same logic as previous that, u being a smooth function of r , denominator $\mathcal{D} = 0$ implies numerator \mathcal{N} has to be zero which gives us the condition for critical point.

$\mathcal{D} = 0$ implies that the critical point coincides with sonic point, i.e.

$$u|_{r_c} = c_s \quad (63)$$

Similarly, from $\mathcal{N} = 0$, the full critical condition can be derived as

$$u_c = c_s|_{r_c} = \sqrt{\frac{2\lambda^2(r - 2)^2 - 2r^3}{(2r^3 - 2\lambda^2r + 4\lambda^2)(3 - 2r)}} \quad (64)$$

Simplifying (64) we get a 4th order polynomial in r_c as:

$$f(r_c) = 4r_c^4c_s^2 - 2r_c^3(3c_s^2 + 1) - 2\lambda^2r_c^2(2c_s^2 - 1) + 2\lambda^2r_c(7c_s^2 - 4) - 4\lambda^2(3c_s^2 - 2) \quad (65)$$

Now doing the same analysis as the aforementioned way, we have got a bifurcation curve in λ - T space taking the range of r from $3.1 r_s$ to $10,000 r_s$ for the specified range of λ and T . The respective diagram is shown in 6.

In 6, the region I denotes the mono-critical region where only one critical point exists and region II denotes the multi-critical region where three critical points exist. Here, OA line represents the left boundary(from region I to II) and OB line represents the right boundary(from region II to I). OAB region(bounded by OA and OB lines) specifies the multi-critical region II. Now, for example, at $T = 6.0 \times 10^{10}$, in the range of $0 \leq \lambda \leq 3.52$ (region I) there is a mono-critical solution of $f(r_c)$ and in the range $3.52 \leq \lambda \leq 3.81$ there is a multi-critical solution of $f(r_c)$ (region II) and in the range $3.81 \leq \lambda \leq 4.0$ there again exists a mono-critical solution of $f(r_c)$ (region I).

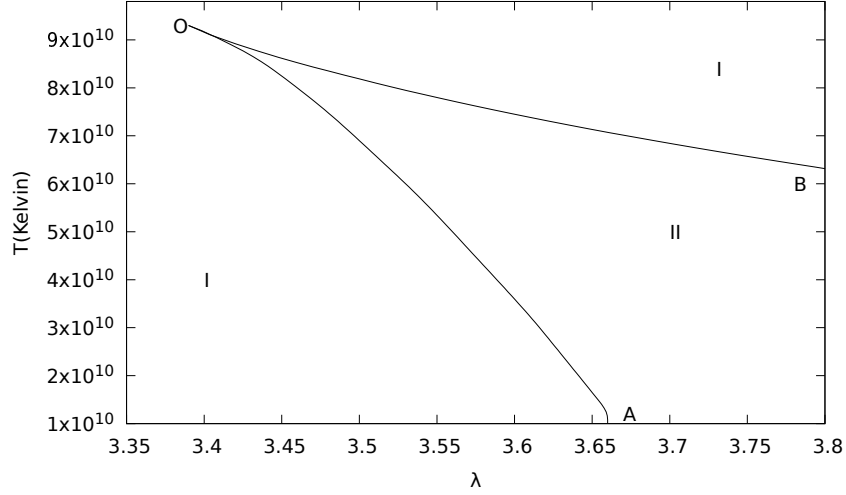


Figure 6: Isothermal accretion in conical disc and related bifurcation phenomena

5.3 Flow in vertical hydrostatic equilibrium

5.3.1 Abramowicz-Lanza-Percival Model

The mass accretion rate for this accretion disc geometry is given by,

$$\dot{M} = 2\pi\rho r \frac{u\sqrt{1-\frac{2}{r}}}{\sqrt{1-u^2}} 2H(r)^{iso} \quad (66)$$

where $H(r)^{iso}$ denotes the half-thickness of the accretion disc. The expression of $H(r)^{iso}$ is given by,

$$H(r)^{iso} = rc_s \frac{\sqrt{2(1-u^2)(r^3-\lambda^2(r-2))}}{\lambda\sqrt{r-2}} \quad (67)$$

Substituting the value of $H(r)^{iso}$ from equation (67) into equation (66) we obtain the final expression of mass accretion rate \dot{M} as,

$$\dot{M} = 4\pi\rho r^{\frac{3}{2}} \frac{uc_s\sqrt{2(r^3-\lambda^2(r-2))}}{\lambda} \quad (68)$$

Using (68) and (53), we obtain,

$$\frac{du}{dr} = \frac{u(u^2-1)[r^3-\lambda^2(r-2)^2+c_s^2(2-r)(3r^3-2\lambda^2r+3\lambda^2)]}{r(r-2)(r^3-\lambda^2r+2\lambda^2)[u^2(c_s^2+1)-c_s^2]} = \frac{\mathcal{N}}{\mathcal{D}} \quad (69)$$

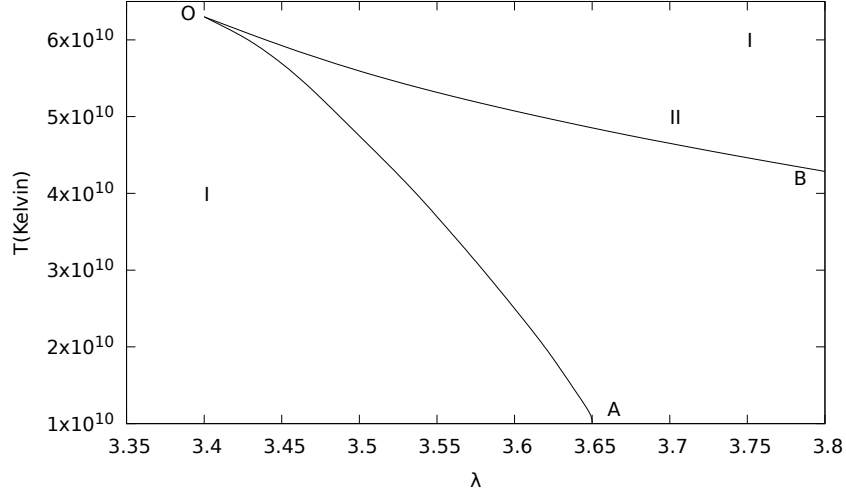


Figure 7: Isothermal accretion in ALP flow model and related bifurcation phenomena

As u is a continuous function of r , by the above mentioned argument, $\mathcal{D} = 0$ implies numerator \mathcal{N} must be zero. Here, $\mathcal{D} = 0$ gives us,

$$u|_{r_c} = \frac{c_s}{\sqrt{1 + c_s^2}} \quad (70)$$

And the other critical point condition is obtained from $\mathcal{N} = 0$ as,

$$c_s|_{r_c} = \sqrt{\frac{\lambda^2(r-2)^2 - r^3}{(2-r)(3r^3 - 2\lambda^2r + 3\lambda^2)}} \quad (71)$$

By putting (70) into (71) and simplifying the whole expression, we get a 4th order polynomial of r_c as:

$$f(r_c) = 6r_c^4 c_s^2 + r_c^3 (-12c_s^2 - 2) + r_c^2 (2\lambda^2 - 4\lambda^2 c_s^2) + r_c (14\lambda^2 c_s^2 - 8\lambda^2) + (8\lambda^2 - 12\lambda^2 c_s^2) \quad (72)$$

We know that, the number of critical points is equal to the number of real roots of the above polynomial. Now applying sturm analysis on (72), for the region $r = 3.1 r_s$ to $10,000 r_s$, we have drawn a bifurcation diagram in λ - T space to describe the flow qualitatively. The respective diagram is shown in the 7.

In 7, the region I denotes the mono-critical region where only one critical point exists and region II denotes the multi-critical region where three critical points exist. Here, OA line rep-

resents the left boundary(from region I to II) and OB line represents the right boundary(from region II to I). OAB region(bounded by OA and OB lines) specifies the multi-critical region II. Now, for example, at $T = 4.0 \times 10^{10}$, in the range of $0 \leq \lambda \leq 3.51$ (region I) there is a mono-critical solution of $f(r_c)$ and in the range $3.51 \leq \lambda \leq 3.83$ there is a multi-critical solution of $f(r_c)$ (region II) and in the range $3.83 \leq \lambda \leq 4.0$ there again exists a mono-critical solution of $f(r_c)$ (region I).

5.3.2 Novikov-Thorne Accretion Flow Model

Here the mass accretion rate is given by,

$$\dot{M} = 4\pi\rho r \frac{u\sqrt{1-\frac{2}{r}}}{\sqrt{1-u^2}} H(r) \quad (73)$$

where expression of disc height $H(r)$ is given by,

$$H(r) = c_s r^{\frac{3}{2}} \frac{\sqrt{1-\frac{3}{r}}}{\sqrt{1-\frac{2}{r}}} \quad (74)$$

Substituting (74) into (73), the mass accretion rate is obtained as,

$$\dot{M} = 4\pi\rho c_s r^{\frac{5}{2}} \frac{u\sqrt{1-\frac{3}{r}}}{\sqrt{1-u^2}} \quad (75)$$

which remains approximately constant throughout the flow.

Using (75) and (53) we obtain,

$$\begin{aligned} \frac{du}{dr} = & \frac{u(1-u^2)[2r^3(r-3) - 2\lambda^2(r^3 - 7r^2 + 16r - 12) - c_s^2 r^3(5r-12)(r-2)]}{2r(2-r)(r-3)(r^3 - \lambda^2 r + 2\lambda^2)(u^2 - c_s^2)} \\ & + \frac{u(1-u^2)[\lambda^2 c_s^2(5r^3 - 32r^2 + 68r - 48)]}{2r(2-r)(r-3)(r^3 - \lambda^2 r + 2\lambda^2)(u^2 - c_s^2)} = \frac{\mathcal{N}}{\mathcal{D}} \end{aligned} \quad (76)$$

Here, we also use aforementioned argument that, as u is a smooth function of r , null value of denominator \mathcal{D} implies that, numerator \mathcal{N} has to be zero which gives us the criticality condition

Inspecting denominator \mathcal{D} we can say that, zero value of \mathcal{D} concludes that, for Novikov-Thorne model also, critical point coincides with sonic point:

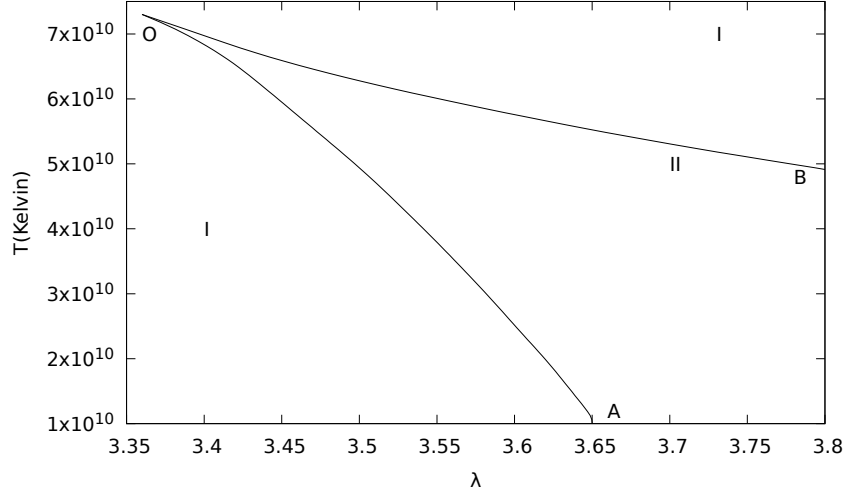


Figure 8: Isothermal accretion in NT flow model and related bifurcation phenomena

$$u|_{r_c} = c_s \quad (77)$$

And $\mathcal{N} = 0$ gives us the actual criticality condition as:

$$u_c = c_s|_{r_c} = \sqrt{\frac{2r^3(r-3) - 2\lambda^2(r^3 - 7r^2 + 16r - 12)}{r^3(5r-12)(r-2) - \lambda^2(5r^3 - 32r^2 + 68r - 48)}} \quad (78)$$

Now simplifying the above expression (78) we get a 5th order polynomial in r_c as:

$$\begin{aligned} f(r_c) = & r_c^3 (-5.\lambda^2 c_s^2 + 24.c_s^2 + 2.\lambda^2 + 6.) + r_c^2 (32.\lambda^2 c_s^2 - 14.\lambda^2) \\ & + r_c (32.\lambda^2 - 68.\lambda^2 c_s^2) + 5.r_c^5 c_s^2 - r_c^4 (22.c_s^2 + 2.) + (48.\lambda^2 c_s^2 - 24.\lambda^2) \end{aligned} \quad (79)$$

Now, we know that, the number of critical points equals to the number of real roots of the above polynomial. Applying sturm analysis on above polynomial (79), for the region $r = 3.1 r_s$ to $10,000 r_s$, we have got a bifurcation diagram in λ - T space to describe the accretion flow qualitatively. The respective diagram is shown in the 8.

In 8, the region I denotes the mono-critical region where only one critical point exists and region II denotes the multi-critical region where three critical points exist. Here, OA line represents the left boundary (from region I to II) and OB line represents the right boundary (from region II to I). OAB region (bounded by OA and OB lines) specifies the multi-critical region

II. Now, for example, at $T = 5.0 \times 10^{10}$, in the range of $0 \leq \lambda \leq 3.50$ (region I) there is a mono-critical solution of $f(r_c)$ and in the range $3.50 \leq \lambda \leq 3.78$ there is a multi-critical solution of $f(r_c)$ (region II) and in the range $3.78 \leq \lambda \leq 4.0$ there again exists a mono-critical solution of $f(r_c)$ (region I).

5.3.3 Riffert–Herold Accretion Flow Model

The mass accretion rate for this RH accretion model is:

$$\dot{M} = 4\pi\rho r \frac{u\sqrt{1 - \frac{2}{r}}}{\sqrt{1 - u^2}} H(r) \quad (80)$$

where disc height $H(r)$ is represented by the following expression,

$$H(r) = 2r^{\frac{3}{2}}c_s\sqrt{1 - \frac{3}{r}} \quad (81)$$

Substituting (81) into (80), we obtain,

$$\dot{M} = 8\pi\rho c_s r^{\frac{5}{2}} \frac{u\sqrt{(1 - \frac{2}{r})(1 - \frac{3}{r})}}{\sqrt{1 - u^2}} \quad (82)$$

which remains constant throughout the flow.

From the expression of \dot{M} (eq. (80)) and ξ (eq. (53)), by using some basic algebra as previous, we get an expression of $\frac{du}{dr}$ which is following:

$$\begin{aligned} \frac{du}{dr} = & \frac{u(u^2 - 1)(-5r^5c_s^2 + 20r^4c_s^2 + 5\lambda^2r^3c_s^2 - 18r^3c_s^2 - 30\lambda^2r^2c_s^2 + 58\lambda^2rc_s^2 - 36\lambda^2c_s^2)}{r(r - 3)(r - 2)(2\lambda^2 + r^3 - \lambda^2r)(u^2 - c_s^2)} \\ & + \frac{u(u^2 - 1)(24\lambda^2 + 2r^4 - 2\lambda^2r^3 - 6r^3 + 14\lambda^2r^2 - 32\lambda^2r)}{r(r - 3)(r - 2)(2\lambda^2 + r^3 - \lambda^2r)(u^2 - c_s^2)} = \frac{\mathcal{N}}{\mathcal{D}} \end{aligned} \quad (83)$$

Now, as u is a smooth function of r , following the previously argument, zero value of denominator \mathcal{D} at some radial point in the prescribed range implies that, numerator \mathcal{N} has to be zero at those points, which gives us the condition for criticality in the process of accretion.

Observing denominator \mathcal{D} we can say that, from the null value of \mathcal{D} we can conclude that, for Riffert herold model also, critical point is actually the sonic point:

$$u|_{r_c} = c_s \quad (84)$$

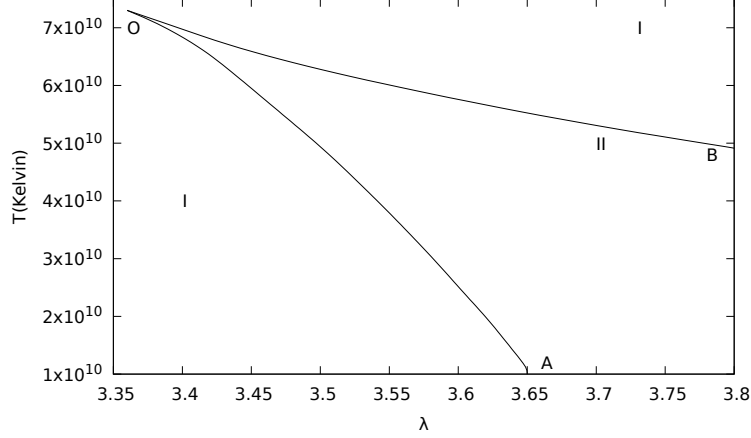


Figure 9: Isothermal accretion in RH flow model and related bifurcation phenomena

and, then from $\mathcal{N} = 0$, we get the required criticality condition as:

$$u_c = c_s \big|_{r_c} = \sqrt{\frac{(24\lambda^2 + 2r^4 - 2\lambda^2 r^3 - 6r^3 + 14\lambda^2 r^2 - 32\lambda^2 r)}{(5r^5 - 20r^4 - 5\lambda^2 r^3 + 18r^3 + 30\lambda^2 r^2 - 58\lambda^2 r + 36\lambda^2)}} \quad (85)$$

Simplifying above equation (85) we get a 5th order polynomial in r_c as follows:

$$\begin{aligned} f(r_c) = & r_c^3 (-5.\lambda^2 c_s^2 + 18.c_s^2 + 2.\lambda^2 + 6.) + r_c^2 (30.\lambda^2 c_s^2 - 14.\lambda^2) \\ & + r_c (32.\lambda^2 - 58.\lambda^2 c_s^2) + 5.r_c^5 c_s^2 - r_c^4 (20.c_s^2 + 2.) + (36.\lambda^2 c_s^2 - 24.\lambda^2) \end{aligned} \quad (86)$$

We know that, the number of critical points is equal to the number of real roots of the above polynomial. Now applying Sturm analysis on above polynomial (86), for the region $r = 3.1 r_s$ to $10,000 r_s$, we have got a bifurcation diagram in λ - T space to describe the accretion flow qualitatively. The respective diagram is shown in the 9.

In 9, the region I denotes the mono-critical region where only one critical point exists and region II denotes the multi-critical region where three critical points exist. Here, OA line represents the left boundary (from region I to II) and OB line represents the right boundary (from region II to I). OAB region (bounded by OA and OB lines) specifies the multi-critical region II. Now, for example, at $T = 5.0 \times 10^{10}$, in the range of $0 \leq \lambda \leq 3.50$ (region I) there is a mono-critical solution of $f(r_c)$ and in the range $3.50 \leq \lambda \leq 3.79$ there is a multi-critical solution of $f(r_c)$ (region II) and in the range $3.79 \leq \lambda \leq 4.0$ there again exists a mono-critical solution of $f(r_c)$ (region I).

Table 2: Bifurcation region for isothermal accretion

Disc geometry	λ	\mathcal{T}
CH	3.67-3.80	$1.5 \times 10^{10} - 1.8 \times 10^{11}$
Quasi-spherical	3.66-3.80	$10^{10} - 1.0 \times 10^{11}$
ALP	3.65-3.80	$10^{10} - 6.50 \times 10^{10}$
NT	3.65-3.80	$10^{10} - 8.0 \times 10^{10}$
RH	3.65 - 3.40	$10^{10} - 8.0 \times 10^{10}$

References

- [1] Liang, E.P.T., Thomson, K.A.: ApJ. 240, 271 (1980)
- [2] Ray, A.K., Bhattacharjee, J.K.: Phys. Rev. E 66, 066303 (2002)
- [3] Afshordi, N., Paczyński, B.: ApJ. 592, 354 (2003)
- [4] Ray, A.K.: MNRAS 344, 83 (2003)
- [5] Ray, A.K.: MNRAS 344, 1085 (2003)
- [6] Ray, A.K., Bhattacharjee, J.K.: A dynamical systems approach to a thin accretion disc and its time-dependent behaviour on large length scales. Eprint arXiv:astro-ph/0511018v1 (2005)
- [7] Ray, A.K., Bhattacharjee, J.K.: Astrophys. J. 627, 368 (2005)
- [8] Chaudhury, S., Ray, A.K., Das, T.K.: MNRAS 373, 146 (2006)
- [9] Ray, A.K., Bhattacharjee, J.K.: Indian J. Phys. 80, 1123 (2006). Eprint arXiv:astro-ph/0703301
- [10] Ray, A.K., Bhattacharjee, J.K.: Class. Quantum Gravity 24, 1479 (2007)
- [11] Bhattacharjee, J.K., Ray, A.K.: ApJ. 668, 409 (2007).
- [12] Goswami, S., Khan, S.N., Ray, A.K., Das, T.K.: MNRAS 378, 1407 (2007)

- [13] Bhattacharjee, J.K., Bhattacharya, A., Das, T.K., Ray, A.K.: MNRAS 398, 841 (2009).
Also at arXiv:0812.4793v1 [astro-ph]
- [14] S. Agarwal, T. K. Das · R. Dey · S. Nag :Gen Relativ Gravit (2012) 44:1637–1655 DOI 10.1007/s10714-012-1358-z
- [15] I. Novikov and K. S. Thorne. Black Holes, ed. De Witt C. & De Witt B. Gordon and Breach, New York, 1973.
- [16] H. Riffert and H. Herold. ApJ, 450:508, 1995
- [17] M. A. Abramowicz, A. Lanza, and M. J. Percival. ApJ, 479:179, 1997.
- [18] Abramowicz, M.A., Zurek, W.H.: ApJ. 246, 314 (1981)
- [19] Blaes, O., 1987. MNRAS 227, 975.
- [20] Muchotrzeb, B., Paczynski, B.: Acta Actron. 32, 1 (1982)
- [21] Muchotrzeb, B.: Acta Astron. 33, 79 (1983)
- [22] Fukue, J.: PASJ 35, 355 (1983)
- [23] Fukue, J.: PASJ 39, 309 (1987)
- [24] Matsumoto, R., Kato, S., Fukue, J., & Okazaki, A. T.: PASJ 36, 1 (1984)
- [25] P. Tarafdar, D. B. Ananda, S. Nag, T. K. Das: Phys. Rev. D 100, 043024 (2019)
- [26] P. Tarafdar, T. K. Das: New Astronomy 62, 1-14 (2018).
- [27] Fukue, J.: PASJ 56, 681 (2004)
- [28] Fukue, J.: PASJ 56, 959 (2004)
- [29] Lu, J.F.: A & A 148, 176 (1985)
- [30] Lu, F.: Gen. Relativ. Gravit. 18, 45L (1986)
- [31] Muchotrzeb-Czerny, B.: Acta Astronomica 36, 1 (1986)
- [32] Abramowicz, M.A., Kato, S.: ApJ. 336, 304 (1989)

- [33] Abramowicz, M.A., Chakrabarti, S.K.: ApJ. 350, 281 (1990)
- [34] Kafatos, M., Yang, R.X.: MNRAS 268, 925 (1994)
- [35] Yang, R.X., Kafatos, M.: A & A 295, 238 (1995)
- [36] Caditz, D.M., Tsuruta, S.: ApJ. 501, 242 (1998)
- [37] Das, T.K.: ApJ. 577, 880 (2002)
- [38] Barai, P., Das, T.K., Wiita, P.J.: ApJ. 613, L49 (2004)
- [39] Abraham, H., Bilić, N., Das, T.K.: Class. Quantum Gravity 23, 2371 (2006)
- [40] Das, T.K., Bilić, N., Dasgupta, S.: JCAP 06, 009 (2007)
- [41] Das, T.K., Czerny, B.: New Astron. 17, 254 (2012)
- [42] Nag, S., Acharya, S., Ray, A.K., Das, T.K.: New Astron. 17, 285 (2012)
- [43] Chakrabarti, S.K.: ApJ. 347, 365 (1989)
- [44] Das, T.K., Pendharkar, J.K., Mitra, S.: ApJ. 592, 1078 (2003)
- [45] Illarionov, A., Sunyaev, R.A.: A & A 39, 205 (1975)
- [46] Liang, E.P.T., Nolan, P.L.: Space. Sci. Rev. 38, 353 (1984)
- [47] Bisikalo, A.A., Boyarchuk, V.M., Chechetkin, V.M., Kuznetsov, O.A., Molteni, D.: MNRAS 300, 39 (1998)
- [48] Illarionov, A.F.: Soviet Astron. 31, 618 (1988)
- [49] Ho, L.C.: In: Chakrabarti, S.K. (ed.) Observational Evidence for Black Holes in the Universe, p. 153 Kluwer, Dordrecht (1999)
- [50] Igumenshchev, I.V., Abramowicz, M.A.: MNRAS 303, 309 (1999)
- [51] Matsumoto, R., Kato, S., Fukue, J., Okazaki, A.T.: PASJ 36, 71 (1984)
- [52] Paczyński, B.: Nature 327, 303 (1987)
- [53] Abramowicz, M.A., Czerny, B., Lasota, J.P., Szuszkiewicz, E.: ApJ. 332, 646 (1988)

- [54] Chen, X., Taam, R.: ApJ. 412, 254 (1993)
- [55] Artemova, I.V., Björnsson, G., Novikov, I.D.: ApJ. 461, 565 (1996)
- [56] Narayan, R., Kato, S., Honma, F.: ApJ. 476, 49 (1997)
- [57] Wiita, P.J. In: Iyer, B.R., Bhawal, B. (eds.) Black Holes, Gravitational Radiation and the Universe, p.249, Kluwer, Dordrecht (1999) Hawley, J.F., Krolik, J.H.: ApJ. 548, 348 (2001)
- [58] Armitage, P.J., Reynolds, C.S., Chiang, J.: ApJ. 648, 868 (2001)
- [59] Abramowicz, M.A., Lanza, A., Percival, M.J.: ApJ. 479, 179 (1997)
- [60] Stark, H.: An Introduction to Number Theory. MIT Press, 1978; ISBN 0-262-69060-8
- [61] Bochnak, J., Coste, M., Roy, M.F.: Real Algebraic Geometry. Springer, Berlin (1991)
- [62] Manmoto T.: APJ 534,734 (2000)

Appendix 1

Sturm Theorem

The number of real roots of an algebraic polynomial with real coefficients whose roots are simple over an interval, the endpoints of which are not roots, is equal to the difference between the number of sign changes of the Sturm chains formed for the interval ends.

Sturm chain – construction:

p — a polynomial with real coefficients, P_i — i th element of the Sturm chain,

$$P_0 = p$$

$$P_1 = p'$$

and for $i \geq 2$

$$P_i = -\text{remainder} \left(\frac{P_{i-2}}{P_{i-1}} \right)$$

The number of real roots in a half-open interval $(a, b]$ of the polynomial \mathcal{P} : $\#(\text{change in sign of } P_i \text{ s at } a) - \#(\text{change in sign of } P_i \text{ s at } b)$.

Appendix 2

The polynomial equation for the polytropic accretion with constant hight disc structure.

$$\sum_{i=0}^{11} a_{ch_i} r_c^i = 0 \quad (87)$$

coefficients:

$$\begin{aligned} a_{ch_0} &= -36\mathcal{E}^2\lambda^6 + 24\mathcal{E}^2\gamma\lambda^6 - 4\mathcal{E}^2\gamma^2\lambda^6 \\ a_{ch_1} &= (84\mathcal{E}^2\lambda^6 - 64\mathcal{E}^2\gamma\lambda^6 + 12\mathcal{E}^2\gamma^2\lambda^6) \\ a_{ch_2} &= (4\lambda^4 - 8\gamma\lambda^4 + 4\gamma^2\lambda^4 - 73\mathcal{E}^2\lambda^6 + 62\mathcal{E}^2\gamma\lambda^6 - 13\mathcal{E}^2\gamma^2\lambda^6) \\ a_{ch_3} &= (-16\lambda^4 + 36\mathcal{E}^2\lambda^4 + 32\gamma\lambda^4 - 12\mathcal{E}^2\gamma\lambda^4 - 16\gamma^2\lambda^4 + 28\mathcal{E}^2\lambda^6 - 26\mathcal{E}^2\gamma\lambda^6 + 6\mathcal{E}^2\gamma^2\lambda^6) \\ a_{ch_4} &= (25\lambda^4 - 72\mathcal{E}^2\lambda^4 - 50\gamma\lambda^4 + 34\mathcal{E}^2\gamma\lambda^4 + 25\gamma^2\lambda^4 - 2\mathcal{E}^2\gamma^2\lambda^4 - 4\mathcal{E}^2\lambda^6 + 4\mathcal{E}^2\gamma\lambda^6 - \mathcal{E}^2\gamma^2\lambda^6) \\ a_{ch_5} &= (4\lambda^2 - 8\gamma\lambda^2 + 4\gamma^2\lambda^2 - 19\lambda^4 + 59\mathcal{E}^2\lambda^4 + 38\gamma\lambda^4 - 38\mathcal{E}^2\gamma\lambda^4 - 19\gamma^2\lambda^4 + 5\mathcal{E}^2\gamma^2\lambda^4) \\ a_{ch_6} &= (-14\lambda^2 + 28\gamma\lambda^2 - 12\mathcal{E}^2\gamma\lambda^2 - 14\gamma^2\lambda^2 + 3\mathcal{E}^2\gamma^2\lambda^2 + 7\lambda^4 \\ &\quad - \mathcal{E}^2\lambda^4 - 14\gamma\lambda^4 + 20\mathcal{E}^2\gamma\lambda^4 + 7\gamma^2\lambda^4 - 4\mathcal{E}^2\gamma^2\lambda^4) \\ a_{ch_7} &= (18\lambda^2 - 12\mathcal{E}^2\lambda^2 - 36\gamma\lambda^2 + 28\mathcal{E}^2\gamma\lambda^2 + 18\gamma^2\lambda^2 - 8\mathcal{E}^2\gamma^2\lambda^2 - \lambda^4 \\ &\quad + 4\mathcal{E}^2\lambda^4 + 2\gamma\lambda^4 - 4\mathcal{E}^2\gamma\lambda^4\gamma^2\lambda^4 + \mathcal{E}^2\gamma^2\lambda^4) \\ a_{ch_8} &= (1 - 2\gamma + \gamma^2 - 10\lambda^2 + 13\mathcal{E}^2\lambda^2 + 20\gamma\lambda^2 - 22\mathcal{E}^2\gamma\lambda^2 - 10\gamma^2\lambda^2 + 7\mathcal{E}^2\gamma^2\lambda^2) \\ a_{ch_9} &= (-3 + 6\gamma - 3\gamma^2 + \mathcal{E}^2\gamma^2 + 2\lambda^2 - 4\mathcal{E}^2\lambda^2 - 4\gamma\lambda^2 + 6\mathcal{E}^2\gamma\lambda^2 + 2\gamma^2\lambda^2 - 2\mathcal{E}^2\gamma^2\lambda^2) \\ a_{ch_{10}} &= (3 - 6\gamma + 2\mathcal{E}^2\gamma + 3\gamma^2 - 2\mathcal{E}^2\gamma^2) \\ a_{ch_{11}} &= (-1 + \mathcal{E}^2 + 2\gamma - 2\mathcal{E}^2\gamma - \gamma^2 + \mathcal{E}^2\gamma^2) \end{aligned}$$

Appendix 3

The polynomial equation for the polytropic accretion with conical disc structure.

$$\sum_{i=0}^{11} a_{qu_i} x^i = 0 \quad (88)$$

coefficients:

$$a_{qu_{10}} = (36 - 16\epsilon^2 - 72\gamma + 40\epsilon^2\gamma + 36\gamma^2 - 24\epsilon^2\gamma^2)$$

$$a_{qu_{11}} = (-8 + 8\epsilon^2 + 16\gamma - 16\epsilon^2\gamma - 8\gamma^2 + 8\epsilon^2\gamma^2)$$

$$a_{qu_0} = (100\epsilon^2\lambda^6 - 120\epsilon^2\gamma\lambda^6 + 36\epsilon^2\gamma^2\lambda^6)$$

$$a_{qu_9} = (-54 + 8\epsilon^2 + 108\gamma - 24\epsilon^2\gamma - 54\gamma^2 + 18\epsilon^2\gamma^2 \\ + 16\lambda^2 - 28\epsilon^2\lambda^2 - 32\gamma\lambda^2 + 48\epsilon^2\gamma\lambda^2 + 16\gamma^2\lambda^2 - 20\epsilon^2\gamma^2\lambda^2)$$

$$a_{qu_8} = (27 - 54\gamma + 27\gamma^2 - 104\lambda^2 + 124\epsilon^2\lambda^2 + 208\gamma\lambda^2 \\ - 224\epsilon^2\gamma\lambda^2 - 104\gamma^2\lambda^2 + 96\epsilon^2\gamma^2\lambda^2)$$

$$a_{qu_6} = (-270\lambda^2 + 84\epsilon^2\lambda^2 + 540\gamma\lambda^2 - 180\epsilon^2\gamma\lambda^2 - 270\gamma^2\lambda^2 + 81\epsilon^2\gamma^2\lambda^2 + 68\lambda^4 - 200\epsilon^2\lambda^4 \\ - 136\gamma\lambda^4 + 290\epsilon^2\gamma\lambda^4 + 68\gamma^2\lambda^4 - 104\epsilon^2\gamma^2\lambda^4)$$

$$a_{qu_7} = (252\lambda^2 - 180\epsilon^2\lambda^2 - 504\gamma\lambda^2 + 348\epsilon^2\gamma\lambda^2 + 252\gamma^2\lambda^2 - 153\epsilon^2\gamma^2\lambda^2 - 8\lambda^4 \\ + 30\epsilon^2\lambda^4 + 16\gamma\lambda^4 - 44\epsilon^2\gamma\lambda^4 - 8\gamma^2\lambda^4 + 16\epsilon^2\gamma^2\lambda^4)$$

$$a_{qu_1} = (-320\epsilon^2\lambda^6 + 392\epsilon^2\gamma\lambda^6 - 120\epsilon^2\gamma^2\lambda^6)$$

$$a_{qu_3} = (-324\lambda^4 + 240\epsilon^2\lambda^4 + 648\gamma\lambda^4 - 324\epsilon^2\gamma\lambda^4 - 324\gamma^2\lambda^4 + 108\epsilon^2\gamma^2\lambda^4 \\ - 0247\epsilon^2\lambda^6 + 316\epsilon^2\gamma\lambda^6 - 101\epsilon^2\gamma^2\lambda^6)$$

$$a_{qu_5} = (108\lambda^2 - 216\gamma\lambda^2 + 108\gamma^2\lambda^2 - 230\lambda^4 + 502\epsilon^2\lambda^4 + 460\gamma\lambda^4 - 716\epsilon^2\gamma\lambda^4 \\ - 230\gamma^2\lambda^4 + 252\epsilon^2\gamma^2\lambda^4 - 9\epsilon^2\lambda^6 + 12\epsilon^2\gamma\lambda^6 - 4\epsilon^2\gamma^2\lambda^6)$$

$$\begin{aligned}
a_{qu_4} &= (387\lambda^4 - 564\epsilon^2\lambda^4 - 774\gamma\lambda^4 \\
&+ 786\epsilon^2\gamma\lambda^4 + 387\gamma^2\lambda^4 - 270\epsilon^2\gamma^2\lambda^4 \\
&+ 75\epsilon^2\lambda^6 - 98\epsilon^2\gamma\lambda^6 + 32\epsilon^2\gamma^2\lambda^6) \\
a_{qu_2} &(108\lambda^4 - 216\gamma\lambda^4 + 108\gamma^2\lambda^4 + 401\epsilon^2\lambda^6 - 502\epsilon^2\gamma\lambda^6 + 157\epsilon^2\gamma^2\lambda^6)
\end{aligned}$$

Appendix 4

The polynomial equation for the polytropic accretion in Novikov Thorne disc.

$$\sum_{i=0}^{15} a_{NT_i} x^i = 0 \quad (89)$$

coefficients:

$$a_{NT_{14}} = (1900 - 3800\gamma + 1900\gamma^2 - 1650\epsilon^2 + 3400\gamma\epsilon^2 - 1750\gamma^2\epsilon^2)$$

$$a_{NT_{15}} = (-125 + 250\gamma - 125\gamma^2 + 125\epsilon^2 - 250\gamma\epsilon^2 + 125\gamma^2\epsilon^2)$$

$$a_{NT_0} = 86400\epsilon^2\lambda^6 - 103680\gamma\epsilon^2\lambda^6 + 31104\gamma^2\epsilon^2\lambda^6$$

$$\begin{aligned}
a_{NT_{13}} &= (-12360 + 24720\gamma - 12360\gamma^2 + 9045\epsilon^2 - 19290\gamma\epsilon^2 + 10265\gamma^2\epsilon^2 + 250\lambda^2 - 500\gamma\lambda^2 + 250\gamma^2\lambda^2 \\
&- 375\epsilon^2\lambda^2 + 650\gamma\epsilon^2\lambda^2 - 275\gamma^2\epsilon^2\lambda^2)
\end{aligned}$$

$$\begin{aligned}
a_{NT_{12}} &= (44608 - 89216\gamma + 44608\gamma^2 - 26334\epsilon^2 + 58404\gamma\epsilon^2 - 32286\gamma^2\epsilon^2 - 4300\lambda^2 + 8600\gamma\lambda^2 - 4300\gamma^2\lambda^2 \\
&+ 5730\epsilon^2\lambda^2 - 10040\gamma\epsilon^2\lambda^2 + 4270\gamma^2\epsilon^2\lambda^2)
\end{aligned}$$

$$a_{NT_{10}} = (124992 - 249984\gamma + 124992\gamma^2 - 37044\epsilon^2 + 90216\gamma\epsilon^2 - 54756\gamma^2\epsilon^2 - 138656\lambda^2 + 277312\gamma\lambda^2 - 138656\gamma^2\lambda^2)$$

$$+136134\epsilon^2\lambda^2 - 245412\gamma\epsilon^2\lambda^2 + 105782\gamma^2\epsilon^2\lambda^2 + 2400\lambda^4 - 4800\gamma\lambda^4 + 2400\gamma^2\lambda^4 \\ - 6210\epsilon^2\lambda^4 + 9264\gamma\epsilon^2\lambda^4 - 3406\gamma^2\epsilon^2\lambda^4)$$

$$a_{NT_{11}} = (-96464 + 192928\gamma - 96464\gamma^2 + 42903\epsilon^2 - 99450\gamma\epsilon^2 + 57423\gamma^2\epsilon^2 + 32320\lambda^2 - 64640\gamma\lambda^2 + 32320\gamma^2\lambda^2 \\ - 37491\epsilon^2\lambda^2 + 66554\gamma\epsilon^2\lambda^2 - 28483\gamma^2\epsilon^2\lambda^2 - 125\lambda^4 + 250\gamma\lambda^4 \\ - 125\gamma^2\lambda^4 + 360\epsilon^2\lambda^4 - 540\gamma\epsilon^2\lambda^4 + 200\gamma^2\epsilon^2\lambda^4)$$

$$a_{NT_3} = (-470016\lambda^4 + 940032\gamma\lambda^4 - 470016\gamma^2\lambda^4 + 168480\epsilon^2\lambda^4 - 243648\gamma\epsilon^2\lambda^4 + 85536\gamma^2\epsilon^2\lambda^4 \\ - 789264\epsilon^2\lambda^6 + 977760\gamma\epsilon^2\lambda^6 - 302736\gamma^2\epsilon^2\lambda^6)$$

$$a_{NT_1} = (-371520\epsilon^2\lambda^6 + 450432\gamma\epsilon^2\lambda^6 - 136512\gamma^2\epsilon^2\lambda^6)$$

$$a_{NT_5} = (110592\lambda^2 - 221184\gamma\lambda^2 + 110592\gamma^2\lambda^2 - 975680\lambda^4 + 1951360\gamma\lambda^4 - 975680\gamma^2\lambda^4 + 1013472\epsilon^2\lambda^4 \\ - 1478016\gamma\epsilon^2\lambda^4 + 525600\gamma^2\epsilon^2\lambda^4 - 268380\epsilon^2\lambda^6 + 340200\gamma\epsilon^2\lambda^6 - 107772\gamma^2\epsilon^2\lambda^6)$$

$$a_{NT_7} = (679680\lambda^2 - 1359360\gamma\lambda^2 + 679680\gamma^2\lambda^2 - 278964\epsilon^2\lambda^2 + 535032\gamma\epsilon^2\lambda^2 - 236628\gamma^2\epsilon^2\lambda^2 - 324336\lambda^4 \\ + 648672\gamma\lambda^4 - 324336\gamma^2\lambda^4 + 544698\epsilon^2\lambda^4 - 801132\gamma\epsilon^2\lambda^4 + 288602\gamma^2\epsilon^2\lambda^4 \\ - 17307\epsilon^2\lambda^6 + 22482\gamma\epsilon^2\lambda^6 - 7299\gamma^2\epsilon^2\lambda^6)$$

$$a_{NT_9} = (-89856 + 179712\gamma - 89856\gamma^2 + 13230\epsilon^2 - 34020\gamma\epsilon^2 + 21870\gamma^2\epsilon^2 + 371360\lambda^2 - 742720\gamma\lambda^2 + 371360\gamma^2\lambda^2 \\ - 296199\epsilon^2\lambda^2 + 543594\gamma\epsilon^2\lambda^2 - 236175\gamma^2\epsilon^2\lambda^2 - 20460\lambda^4 + 40920\gamma\lambda^4 - 20460\gamma^2\lambda^4 + 46863\epsilon^2\lambda^4 \\ - 69558\gamma\epsilon^2\lambda^4 + 25395\gamma^2\epsilon^2\lambda^4 - 108\epsilon^2\lambda^6 + 144\gamma\epsilon^2\lambda^6 - 48\gamma^2\epsilon^2\lambda^6)$$

$$a_{NT_8} = (27648 - 55296\gamma + 27648\gamma^2 - 635840\lambda^2 + 1271680\gamma\lambda^2 - 635840\gamma^2\lambda^2 + 386046\epsilon^2\lambda^2 - 723204\gamma\epsilon^2\lambda^2$$

$$+101648\lambda^4 - 203296\gamma\lambda^4 + 101648\gamma^2\lambda^4 - 202086\epsilon^2\lambda^4 + 298548\gamma\epsilon^2\lambda^4 - 108262\gamma^2\epsilon^2\lambda^4 + 2052\epsilon^2\lambda^6 \\ + 316926\gamma^2\epsilon^2\lambda^2 - 2700\gamma\epsilon^2\lambda^6 + 888\gamma^2\epsilon^2\lambda^6)$$

$$a_{NT_6} = (-414720\lambda^2 + 829440\gamma\lambda^2 - 414720\gamma^2\lambda^2 + 86184\epsilon^2\lambda^2 - 169776\gamma\epsilon^2\lambda^2 + 75816\gamma^2\epsilon^2\lambda^2 + 689280\lambda^4 \\ - 1378560\gamma\lambda^4 + 689280\gamma^2\lambda^4 - 939744\epsilon^2\lambda^4 + 1376256\gamma\epsilon^2\lambda^4 - 492576\gamma^2\epsilon^2\lambda^4 \\ + 85050\epsilon^2\lambda^6 - 109116\gamma\epsilon^2\lambda^6 + 34986\gamma^2\epsilon^2\lambda^6)$$

$$a_{NT_4} = (887040\lambda^4 - 1774080\gamma\lambda^4 + 887040\gamma^2\lambda^4 - 624672\epsilon^2\lambda^4 + 907200\gamma\epsilon^2\lambda^4 - 320544\gamma^2\epsilon^2\lambda^4 + 563976\epsilon^2\lambda^6 \\ - 706608\gamma\epsilon^2\lambda^6 + 221256\gamma^2\epsilon^2\lambda^6)$$

$$a_{NT_2} = (110592\lambda^4 - 221184\gamma\lambda^4 + 110592\gamma^2\lambda^4 + \\ 709344\epsilon^2\lambda^6 - 869184\gamma\epsilon^2\lambda^6 + 266208\gamma^2\epsilon^2\lambda^6)$$